



DECELLULARISED TISSUES OBTAINED BY A CO₂-PHILIC DETERGENT AND SUPERCRITICAL CO₂

J. Antons^{1,3}, M.G.M. Marascio², P. Aeberhard^{1,3,†}, G. Weissenberger¹, N. Hirt-Burri³, L.A. Applegate³, P.E. Bourban² and D.P. Pioletti^{1,*}

¹Laboratory of Biomechanical Orthopaedics, Institute of Bioengineering, EPFL, Lausanne, Switzerland

²Laboratory of Processing of Advanced Composites, Institute of Material Science, EPFL, Lausanne, Switzerland

³Regenerative Therapy Unit, Lausanne University Hospital (CHUV), Lausanne, Switzerland

[†]Deceased

Abstract

Tissue decellularisation has gained much attention in regenerative medicine as an alternative to synthetic materials. In decellularised tissues, biological cues can be maintained and provide cellular environments still unmet by synthetic materials. Supercritical CO₂ (scCO₂) has recently emerged as a promising alternative decellularisation technique to aggressive detergents; in addition, scCO₂ provides innate sterilisation. However, to date, decellularisation with scCO₂ is limited to only a few tissue types with low cellular density.

In the current study, a scCO₂ technique to decellularise high density tissues, including articular cartilage, tendon and skin, was developed. Results showed that most of the cellular material was removed, while the sample structure and biocompatibility was preserved. The DNA content was reduced in cartilage, tendon and skin as compared to the native tissue. The treatment did not affect the initial tendon elastic modulus [reduced from 126.35 ± 9.79 MPa to 113.48 ± 8.48 MPa ($p > 0.05$)], while it reduced the cartilage one [from 12.06 ± 2.14 MPa to 1.17 ± 0.34 MPa ($p < 0.0001$)]. Interestingly, cell adhesion molecules such as fibronectin and laminin were still present in the tissues after decellularisation. Bovine chondrocytes were metabolically active and adhered to the surface of all decellularised tissues after 1 week of cell culture. The developed method has the potential to become a cost-effective, one-step procedure for the decellularisation of dense tissues.

Keywords: Decellularisation, supercritical carbon dioxide, extracellular matrix, articular cartilage, tendon, skin.

***Address for correspondence:** Dominique P. Pioletti, PhD, EPFL/STI/IBI/LBO, Station 9, 1015 Lausanne, Switzerland.

Fax number: +41 216938660

Email: dominique.pioletti@epfl.ch

Copyright policy: This article is distributed in accordance with Creative Commons Attribution Licence (<http://creativecommons.org/licenses/by-sa/4.0/>).

Introduction

Decellularised tissue matrices closely mimic their 3D native structures and, thus, have a substantial advantage when compared to synthetic materials. The potential of decellularised matrices is well recognised for the replacement of different tissue types (Badylak *et al.*, 2011; Caione *et al.*, 2012; Macchiarini *et al.*, 2008; Patton *et al.*, 2007). Remarkable success is demonstrated in *in vitro* experiments in which the tissue function of porcine heart (Ott *et al.*, 2008; Wainwright *et al.*, 2010), rat and human kidney (Song *et al.*, 2013) and rat lung (Ott *et al.*, 2010; Petersen *et al.*, 2010) can partly be restored after recellularisation of previously decellularised tissues. Moreover,

decellularised matrices are attractive scaffolds for the repair of tendons (Nourissat *et al.*, 2015; Raghavan *et al.*, 2012; Xu *et al.*, 2017) and cartilage (Sutherland *et al.*, 2014; Yang *et al.*, 2010).

A tissue is considered as decellularised if no visible nuclei remain, less than 50 ng double-stranded DNA per mg extracellular matrix (ECM) dry weight is detected and the DNA fragment length is less than 200 bp (Crapo *et al.*, 2011). Decellularised matrices are produced by a multistep tissue-specific decellularisation process including lysis of the cell membranes, separation of the cellular components from the ECM, solubilisation of the cytoplasmic and nuclear components and removal of the cellular debris (Aubin *et al.*, 2013). However, this decellularisation

process is time-consuming and can compromise the structure and mechanical properties of the tissue (Crapo *et al.*, 2011).

One of the currently most effective decellularisation methods uses perfusion of detergents, such as sodium dodecyl sulphate (SDS), to facilitate removal of cellular material (Ott *et al.*, 2008; Ott *et al.*, 2010; Petersen *et al.*, 2010; Uygun *et al.*, 2010; Wainwright *et al.*, 2010). However, this is limited to vascularised tissues. To decellularise denser tissues, *e.g.* articular cartilage, many steps, such as freeze-thaw, osmotic shock and enzymatic treatment, are required to make the ECM accessible to decellularisation agents. One of the reasons for the long procedure is that this process still relies on the relatively slow diffusion of detergents inside non- or poorly vascularised tissues. Consequently, traces of these detergents might remain inside the tissue and may cause cytotoxicity and adverse effects (Ott *et al.*, 2008). Moreover, at the end of the treatment, the decellularised tissues still have to be sterilised, thus introducing an additional step in the protocol. Sterilisation can be achieved by soaking the decellularised tissues in acids or alcohols (Hodde and Hiles, 2002), ethylene oxide, gamma irradiation (Freytes *et al.*, 2008) or other methods that can further alter the ECM and its mechanical properties (Freytes *et al.*, 2008; Rosario *et al.*, 2008; Sun and Leung, 2008).

One possibility for integrating both sterilisation and decellularisation in one step while simultaneously overcoming diffusion limitations would be the use of a supercritical fluid as a rinsing agent. A supercritical fluid is a substance at a temperature and pressure higher than its critical point, in which liquid and gas phases cannot be distinguished. Supercritical fluids can diffuse through solids as a gas and dissolve substances as a liquid. This unique behaviour could potentially widely reduce decellularisation time by enhancing the diffusion kinetics. A suitable supercritical fluid for decellularisation is supercritical carbon dioxide (scCO₂) since its supercritical point is reached at relatively mild conditions (7.2 MPa/37 °C). Furthermore, scCO₂ can sterilise the sample, having a minor to negligible influence on the tissue structure (Bernhardt *et al.*, 2015). Nevertheless, scCO₂ itself is apolar, thus, the addition of an entrainer, *e.g.* ethanol, is necessary to eliminate or counteract charged molecules such as phospholipids (Dunford and Temelli, 1995; Montanari *et al.*, 1999; Tanaka *et al.*, 2004). Using scCO₂ with ethanol already provides successful decellularisation for aorta, cornea, oesophagus and adipose tissues (Casali *et al.*, 2018; Guler *et al.*, 2017; Halfwerk *et al.*, 2018; Huang *et al.*, 2017; Sawada *et al.*, 2008; Wang *et al.*, 2017; Zambon *et al.*, 2016). However, when dealing with denser tissues, ethanol does not have the required counteractive solvent strength. Instead of ethanol, CO₂-philic detergents, such as the commercially available and low-cost Dehypon® LS-54 (BASF, Ludwigshafen, Germany), could provide the required solvent strength. LS-54 can dissolve bio-macromolecules within scCO₂ and

has a solvability as high as 4 weight % due to its four CO₂-philic propylene oxide groups (Liu *et al.*, 2002).

This study hypothesis was that the detergent LS-54, in combination with scCO₂, might be beneficial for decellularisation of dense tissues. Thus, the purpose of the study was to determine whether the treatment of high density tissues, including articular cartilage, tendon and skin, with a CO₂-philic detergent and a rinsing step in scCO₂ might create a decellularised tissue showing: (i) effective removal of immunological material (visual cell nuclei and DNA), (ii) mechanical and structural properties in the range of the native tissues (control) and (iii) the ability to support cellular growth.

Materials and Methods

Each of the tissues was treated according to the decellularisation procedure summarised in Fig. 1. The tissue-specific protocol and all characterisation techniques are detailed in this section. All products used in the experiments were purchased from Sigma-Aldrich unless mentioned otherwise.

Pre-treatment

Cartilage

Bovine articular cartilage was obtained from a local slaughterhouse and immediately processed on ice to avoid degradation. The cartilage was carefully harvested from the femoral condyles using an 8 mm biopsy punch and a scalpel to create a cylindrical shape. The bone-facing part of the cartilage was removed with a razor blade and a custom-made guide, leaving a uniform 3 mm-thick cylindrical sample. Afterwards, the cartilage cylinders were thoroughly rinsed in phosphate-buffered saline (PBS), dried with a paper towel and stored at -80 °C until further use. As the first tests revealed that it was impossible to completely decellularise cartilage and skin with scCO₂ and detergent only in the autoclave available for the study, additional pre-treatment steps were introduced.

The pre-treatment of cartilage consisted of several steps (Fig. 1). First, 6 freeze-thaw cycles at -80 °C for 2 h (including the initial storage at -80 °C) and, then, at 37 °C for 1 h were performed. Next, the samples were treated with 0.05 % trypsin-EDTA (25300062; Life Technologies) at 37 °C for 24 h. Subsequently, the samples were exposed to an osmotic shock by placing them in hypertonic buffer solution (1.5 M NaCl in 10 mM Tris-HCL, pH 8) for 4 h followed by a hypotonic solution (10 mM Tris-HCL, pH 7.6) for 20 h. Then, the cartilage was immediately treated according to the section "scCO₂ treatment".

Tendons

Horse superficial digital flexor tendons were purchased from a local slaughterhouse and processed frozen, to avoid degradation, into 2 mm-thick slices using a diamond band saw (Exakt Technologies,

Oklahoma City, Oklahoma, USA). Then, tendons were dried with a paper towel and stored at -80°C until further use.

Skin

Human skin was obtained from the DAL/CHUV biobank (Lausanne, Switzerland), under anonymous donation, in accordance with its regulation and approval by the Institutional Biobank (Lausanne, Switzerland). The human skin was immediately cut into pieces of approximately 15×15 mm, dried with a paper towel and stored at -80°C until further use. To start the decellularisation procedure, skin was pre-treated with 1 M NaCl for 24 h prior to careful removal of the epidermis with forceps. Then, the skin was immediately treated according to the section "scCO₂ treatment".

scCO₂ treatment

Based on the protocols described by others (Guler *et al.*, 2017; Huang *et al.*, 2017; Sawada *et al.*, 2008; Wang *et al.*, 2017), scCO₂ was used to eliminate cellular components from the tissues (Fig. 1). A modification

of these protocols was carried out by pre-saturating the tissues in a CO₂-philic detergent instead of using ethanol as entrainer to add polarity to CO₂. Briefly, all tissues were washed for 24 h in a solution of 2 % LS-54 (Dehypon[®], BASF, Ludwigshafen, Germany) under vigorous shaking at 37°C . Then, the detergent-saturated tissues were individually sealed inside sterilisation bags (Medline Industries, Northfield, Illinois, USA) and placed in an autoclave (SITEC AG, Maur, Switzerland) for 1 h. 99.9 % pure CO₂ was introduced into the pressure vessel (volume of vessel: 4 L), then, pressure was increased to 25 MPa using a high-pressure pump. The temperature was adjusted to 37°C , but the temperature fluctuated between 31 – 37°C due to an imprecise temperature controller, which was conceived for higher temperatures (up to 350°C). Later, the pressure vessel was rapidly depressurised using a manual valve at a depressurisation rate of approximately ~ 10 MPa/min. To remove residual detergent, the samples were washed in PBS under vigorous agitation for 24 h while changing the PBS every 8 h.

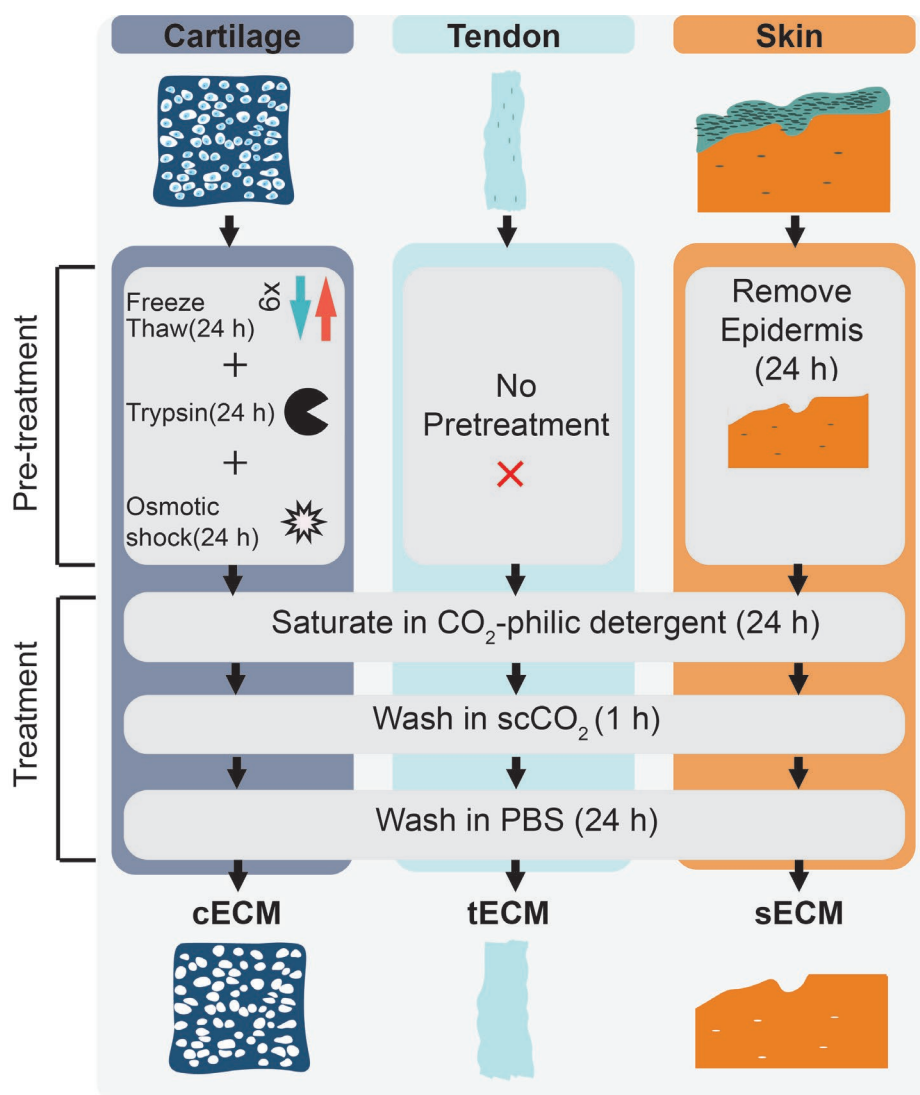


Fig. 1. Scheme of the decellularisation procedure.

Biological characterisation

Histology and immunohistochemistry

To qualitatively assess the removal of cellular material and ECM components, histological sections of native (control) and decellularised tissues (cartilage: cECM; tendon: tECM; skin: sECM) were compared. Briefly, all samples were fixed in 4 % paraformaldehyde and dehydrated in a graded series of ethanol. Samples were embedded in paraffin, sectioned with a microtome to a thickness of 5 µm and stained following standard histology protocols. To stain and visualise any possible remaining cell nuclei, a haematoxylin and eosin dye (H&E) and 4',6-diamidino-2-phenylindole (DAPI) staining was used. Glycosaminoglycans (GAG) and collagen (COL) were visualised with alcian blue and picrosirius red dyes, respectively.

To evaluate the preservation of cell adhesion molecules after decellularisation, immunohistochemistry for fibronectin and laminin was performed. Briefly, 5 µm sections of paraffin-embedded samples were de-paraffinised, rehydrated in PBS and permeabilised with a solution of 0.25 % Tween-20 in PBS for 10 min. To expose the ECM molecule's epitopes, samples were digested for 10 min at 37 °C with 4 mg/mL pepsin in 0.01 M HCl. Fibronectin was detected by immunofluorescence, whereas laminin was detected by a peroxidase reaction. Thus, to detect laminin, an additional step to block endogenous peroxidases by Bloxall solution for 10 min was introduced (Bloxall, SP-6000, Vectorlabs, Burlingame, California, USA). To block non-specific antigens, sections prepared for both fibronectin and laminin labelling were treated with 1 % bovine serum albumin solution in PBS at room temperature for 30 min. Laminin was detected by a peroxidase reaction using a polyclonal primary antibody against laminin (1 : 200; L9393) overnight at 4 °C. This was followed by incubation with one drop per section of the horseradish peroxidase (HRP) labelled secondary goat anti-rabbit antibody (ImmPRESS™ HRP anti-rabbit, MP-7401, Vectorlabs). Subsequently, laminin was detected by adding ImmPACT DAB peroxidase (HRP) substrate (SK-4105, Vectorlabs).

Fibronectin was detected by immunofluorescence by using a monoclonal primary antibody against fibronectin (1 : 200; 610077, BD Biosciences) overnight at 4 °C. This was followed by incubation with Alexa Fluor 568 labelled secondary donkey anti-mouse antibody (1 : 100; A10037, Invitrogen) at ambient temperature for 2 h. Tissue sections were examined under a widefield microscope (DM 5500, Leica) (*n* = 3 for control and LS-54).

DNA quantification

To assess total DNA content, samples were dried overnight in an oven at 65 °C and the dry weight was recorded. Then, the samples were thoroughly digested in papain buffer [100 mM Na₂HPO₄, 100 mM ethylenediaminetetraacetic acid (EDTA), 10 mM cysteine-HCl, 250 µg papain/mL, pH 6.5] at 65 °C

under agitation at 750 rpm overnight or until no visible tissue material remained. The resulting digest was purified by phenol : chloroform : isoamylalcohol (25 : 24 : 1, v/v). The aqueous phase was ethanol-precipitated on ice for 30 min. After centrifugation (16,000 ×g, 10 min, 4 °C), the DNA pellet was washed and reconstituted in nuclease-free water. Subsequently, the DNA content was quantified using a NanoDrop spectrophotometer (Thermo Fisher Scientific). Each sample condition (control and LS-54) was measured in quadruplicate.

GAG quantification

Sulphated GAGs were quantified by 1,9-dimethylmethylene blue dye (DMMB) assay. Chondroitin sulphate dilutions from 0 to 100 µg were used to create a standard curve. 100 µL per well of papain-digested tissues at 6 mg dry tissue/mL were pipetted into a 96-well plate in triplicates. Then, the absorbance was measured on a microplate reader (Wallac 1420 Victor2, PerkinElmer) at a wavelength of 595 nm. Afterwards, chondroitin sulphate concentrations were plotted against absorbance creating a standard curve to determine the GAG concentration in the tissue samples. Each sample condition (control and LS-54) was measured in triplicate.

Mechanical and structural characterisation

Scanning electron microscopy (SEM)

To compare the ultrastructure of the tissue before and after the decellularisation treatment, SEM images were acquired. First, the tissues were fixed for 1 h with 1.25 % glutaraldehyde and 1 % tannic acid in a 0.1 M phosphate buffer, pH 7.4. Then, they were washed in PBS and fixed again in 1.0 % osmium tetroxide in PBS for 30 min. Next, tissues were dehydrated in a graded alcohol series followed by critical point drying (CPD300, Leica Microsystems). Subsequently, the samples were coated with a 4 nm-thick layer of osmium using an osmium plasma coater (OPC60, Filgen, Japan). SEM sample preparation and imaging were performed at the EPFL BioEM facility, Lausanne, Switzerland. Images were acquired on a scanning electron microscope (Merlin SEM, Zeiss) at two magnifications, 5,000× and 43,800×, with an accelerating voltage of 1.5 and 1.2 kV, respectively. Articular cartilage was imaged from the superficial layer (top view), tendons from the top and skin from the cross-section. Each sample condition (control and LS-54) was imaged in triplicate.

Compression and tension tests: cartilage

To assess the difference in elastic modulus between native (control) and decellularised samples (cECM), an unconfined compression test was performed on a uniaxial test system (Instron E3000, Norwood, Massachusetts, USA; load cell: 3 kN). Briefly, each cartilage cylinder (8 mm diameter, 3 mm height) was compressed to 20 % strain at a compression rate of 200 µm/s. The elastic modulus was determined from

the stress-strain curve between 5 and 15 % of strain. The control cartilage was taken from the - 80 °C freezer prior to the compression test and equilibrated to ambient temperature in PBS for 4 h. Each sample condition (control and LS-54) was measured in quadruplicate.

Compression and tension tests: tendon

Biomechanical testing of tendons was performed on a uniaxial test system (Instron E3000, Norwood, Massachusetts, USA; load cell: 3 kN). The samples (2 mm thickness, 50 mm length, 12 mm width) were placed between two standard tensile test clamps: one portion was attached to the upper clamp and the other end to the lower clamp with an initial tendon free length of 20 mm. An elongation rate of 0.1 mm/s was applied. The control tendon was taken from the - 80 °C freezer prior to the tension test and equilibrated to ambient temperature in PBS for 4 h. Each sample condition (control and LS-54) was measured in quadruplicate.

Compression and tension tests: skin

Skin was not mechanically characterised due to its limited load-bearing function.

Biocompatibility

Zone of inhibition assay

To evaluate the biocompatibility of the decellularised tissues, a Zone of Inhibition (ZoI) assay was performed. Thus, the decellularised samples were tightly fixed into a 35 mm cell culture dish using a custom-made stainless-steel clamp. The size of the samples were 8 mm diameter and 3 mm depth for the cartilage plugs, 15 × 12 × 2 mm for tendon and 15 × 15 × 2 mm for skin. The bovine chondrocytes used for the biocompatibility tests were previously extracted from fresh bovine articular cartilage tissue using collagenase extraction. Briefly, the cell extraction was conducted for 24 h with 0.6 % collagenase II (Life Technologies) in Dulbecco's modified Eagle's medium (DMEM) in a humidified atmosphere at 37 °C and 5 % CO₂. Subsequently, DMEM (10 % foetal bovine serum, 2 mM L-glutamine, 100 units/mL penicillin-streptomycin) containing 300,000 bovine chondrocytes (passage 5) was added to the cell culture dish. The cells were cultured in a humidified atmosphere at 37 °C and 5 % CO₂ until full confluence (*i.e.* 100 %) was reached. A Giemsa dye was applied to stain and visualise the chondrocytes surrounding the material and any possible ZoI. Microscopy images for the Giemsa staining were acquired by a Leica DM5500 microscope and overview images were taken by an Iphone 5s (Apple). Each sample condition (control and scCO₂/LS-54) was tested in triplicate.

Cell viability

To determine the cell viability, a PrestoBlue™ assay (PrestoBlue™, A13261, Life Technologies) was performed at day 1 and day 7 following the

manufacturer's instructions. Briefly, 1 million bovine chondrocytes (passage 5) in 50 µL DMEM were evenly pipetted on top of the tissues and left to attach for 1 h in a humidified atmosphere at 37 °C and 5 % CO₂. Then, DMEM was added to fully immerse the sample. The medium was changed every other day and at day 1 and day 7 a PrestoBlue™ assay was performed. Therefore, a 10 % mixture of PrestoBlue™ reagent in DMEM was prepared and added to the chondrocytes. After 2 h incubation time, 100 µL supernatant per well was distributed in triplicate in a black 96-well plate. Then, the fluorescence at 595 nm was measured using a microplate reader (Wallac 1420 Victor2, PerkinElmer).

To visualise metabolically active cells on the acellular tissues, a MTT assay (MTT, M6494, Thermo Fisher Scientific) was carried out following the manufacturer's protocol. Thus, 1 million bovine chondrocytes (passage 5) in 50 µL DMEM were evenly pipetted on top of the tissues and left to attach for 1 h in a humidified atmosphere at 37 °C and 5 % CO₂. Then, DMEM was carefully added to fully immerse the tissues. The medium was changed every other day. At day 7, a MTT assay was performed for 4 h at 37 °C in a humidified atmosphere containing 5 % CO₂ using a 10 % mixture of MTT reagent and DMEM. Next, cell penetration was evaluated by histology, following fixing in 4 % paraformaldehyde and embedding in paraffin. 5 µm-thick sections of the tissues were prepared by a microtome and stained by H&E to visualise cell penetration by staining of cell nuclei. Microscopy images for the MTT assay and cell penetration were acquired by a Leica DM5500 microscope and the overview images were taken by an Iphone 5s (Apple). Each sample condition (control and scCO₂/LS-54) was tested in triplicate.

Statistics

Statistical analysis was performed using GraphPad Prism (La Jolla, CA, USA) software. Means and standard errors were provided for DNA, GAG quantification and mechanical properties. An unpaired two-tailed student's *t*-test was used to compare differences between native (control) and decellularised tissues (cECM, tECM, sECM). *p* ≤ 0.05 was considered statistically significant.

Results

Biological characterisation

Histology

H&E staining showed complete removal of cell nuclei from articular cartilage, tendons and skin, whereas trace amounts of broken cell nuclei were detected by DAPI staining (Fig. 2a-c). Picrosirius red staining showed the conservation of collagen (COL), with no visual difference between the control and decellularised tissues. In contrast, GAG content was severely reduced, as evidenced by alcian blue staining.

The preservation of important cell adhesion molecules (fibronectin, laminin) was evaluated by immunohistochemistry. Fibronectin and laminin were still present after the decellularisation procedure (Fig. 3). Articular cartilage was positive for fibronectin in the superficial layer (Fig. 3a, white arrow), however, after decellularisation, fibronectin was distributed in the entire ECM. In both tendons and skin, fibronectin was abundant around the blood vessels (Fig. 3b,c). Laminin was present in the pericellular space (Fig. 3a, black arrow) and around the blood vessels (Fig. 3b,c) and in the basal lamina of native (control) skin (Fig. 3c, red arrow). For the skin (Fig. 3c), it should be emphasised that the epidermis was removed during the decellularisation procedure and, thus, the basal lamina was not present.

DNA and GAG content

DNA content was significantly ($*p < 0.05$) reduced from 1321 ± 210 ng to 241 ± 45 ng dsDNA/mg dry tissue in cartilage (reduced by 82 ± 3 %), from 1135 ± 262 ng to 378 ± 68 ng dsDNA/mg dry tissue in tendons (reduced by 67 ± 6 %) and from 554 ± 34 ng to

29 ± 0.05 ng dsDNA/mg dry tissue in skin (reduced by 95 ± 0.004 %), compared to the native tissue (Fig. 4a,b). GAG content was also severely reduced ($*p < 0.05$) as evidenced by alcian blue staining and quantitative analysis. In cartilage, GAG content was reduced from 294 ± 19 μ g to 68 ± 31 μ g/mg dry tissue (reduced by 87 ± 6 %). In tendons, GAG content was reduced from 21 ± 3 μ g to 6 ± 3 μ g/mg dry tissue (reduced by 70 ± 6 %) and in skin from 4 ± 2 μ g to 2 ± 0.03 μ g/mg dry tissue (reduced by 66 ± 0.4 %), compared to the native tissue (Fig. 4a,b).

Effect of pre-treatment and scCO₂ only

Fig. 8 displays the effects of scCO₂ only and of pre-treatment on the DNA content of cartilage, tendons and skin. Using scCO₂ only did not show any DNA reduction in cartilage (1453 ± 463 ng DNA/mg dry tissue), tendon (1117 ± 34 ng DNA/mg dry tissue) and skin (637 ± 19 ng DNA/mg dry tissue). Likewise, no visual removal of cell nuclei could be detected by histology (H&E staining). Without a pre-treatment, the DNA content of cartilage was not reduced (1363 ± 87 ng DNA/mg dry tissue), whereas it was

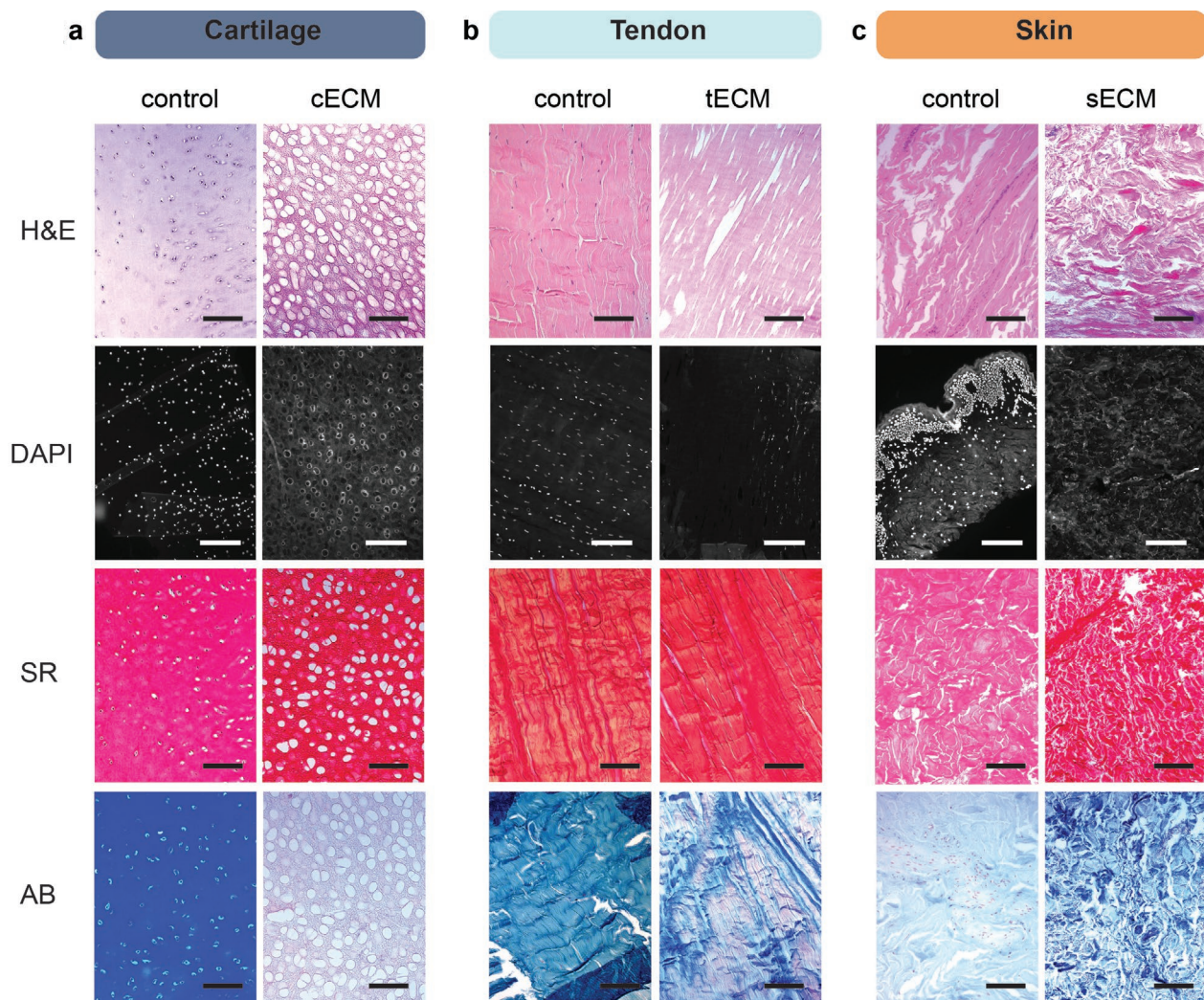


Fig. 2. Histological analysis of tissues before (control) and after decellularisation treatment. Histological sections of (a) bovine cartilage, (b) horse tendon and (c) human skin stained with H&E, DAPI, picrosirius red (SR) and alcian blue (AB) dyes; scale bar: 200 μ m (cartilage: cECM; tendon: tECM; skin: sECM).

significantly reduced in tendons (378 ± 68 ng DNA/mg dry tissue, $*p < 0.05$) and skin (219 ± 13 ng/mg dry tissue, $*p < 0.05$). However, removing the epidermis prior to decellularisation could further reduce the DNA content of the skin (29 ± 0.05 ng DNA/mg dry tissue, Fig. 4a,b) and the number of cell nuclei at a visual analysis.

Mechanical and structural characterisation

SEM

The ultrastructure of the tissues was modified by the decellularisation treatment (Fig. 5). For cartilage (cECM), ECM density appeared particularly low as compared to native tissue (Fig. 5a). This was evident from the decrease in mass surrounding the collagen network. No visual changes in density were observed for tendons and skin. For all tissues, the orientation and size of the collagen fibres themselves matched the control sample almost identically but showed a somewhat looser arrangement.

Compression and tension test

The decellularisation procedure reduced significantly the elastic modulus of articular cartilage ($p < 0.0001$) from 12.06 ± 2.14 MPa to 1.17 ± 0.34 MPa (maintaining 14.44 ± 2.81 % of the original elastic modulus) (Fig. 6a). In contrast, tendon elastic modulus (Fig. 6b) was reduced ($p > 0.05$) from 126.35 ± 9.79 MPa to 113.48 ± 8.48 MPa (maintaining 88.93 ± 7.47 % of its original elastic modulus) after decellularisation.

Biocompatibility

Consistent growth of bovine chondrocytes in direct proximity to the decellularised tissues indicated no ZoI (Fig. 7, top). Other specific cells, including tenocytes and skin fibroblasts, showed similar results for each tissue (data not shown).

Chondrocytes were metabolically active and adhered to the surface of all decellularised tissues after 1 week of cell culture, as evidenced by MTT assay (Fig. 7, middle). The cell penetration of

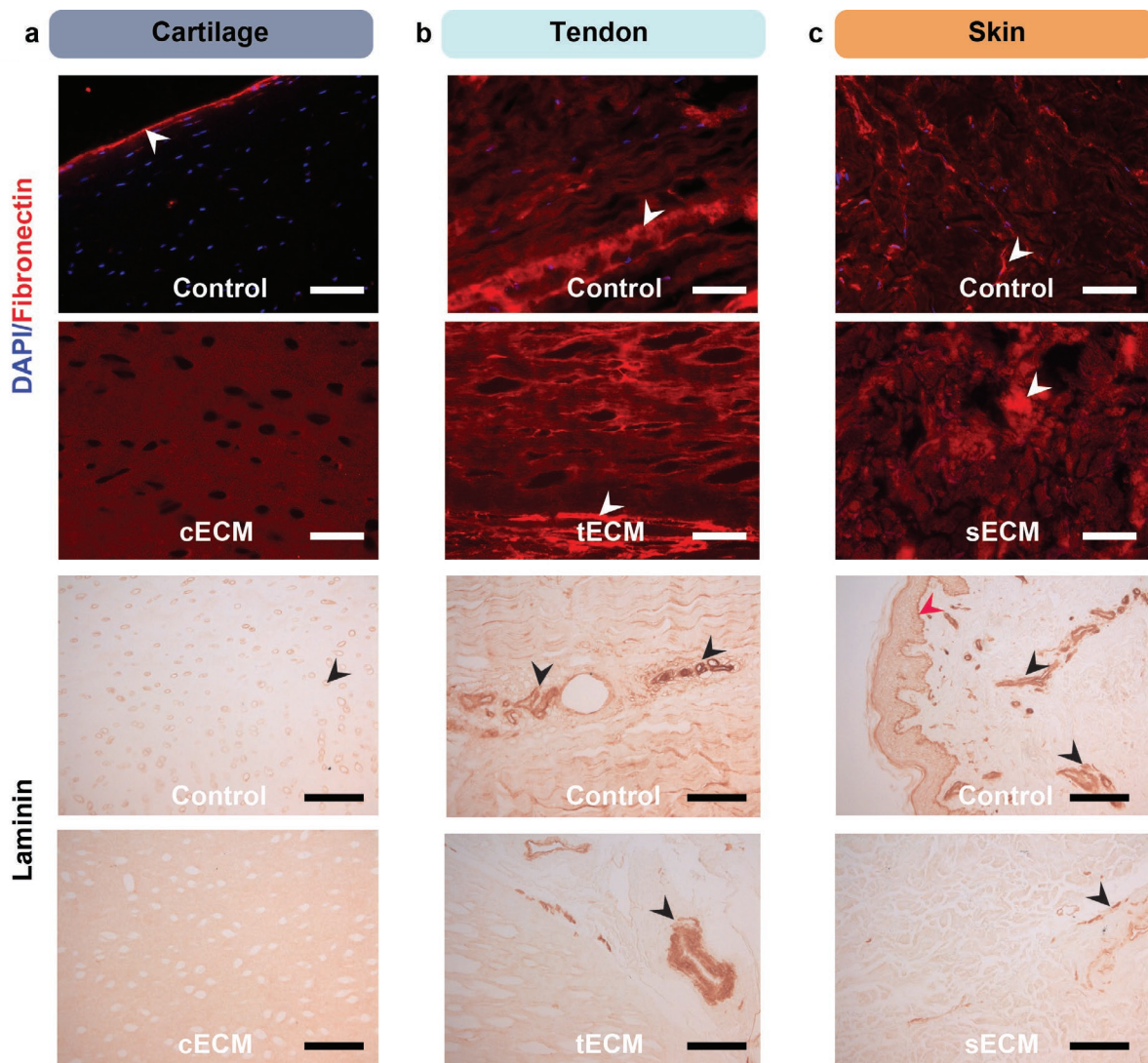


Fig. 3. Cell adhesion molecules retained in the ECM before (control) and after (cECM, tECM, sECM) decellularisation. Histological sections of (a) bovine cartilage, (b) horse tendon and (c) human skin. Fibronectin was visualised by fluorescence whereas laminin was detected by a peroxidase reaction. Arrows indicate regions of high staining intensity, mostly around blood vessels and in the pericellular space; scale bar: 200 μ m.

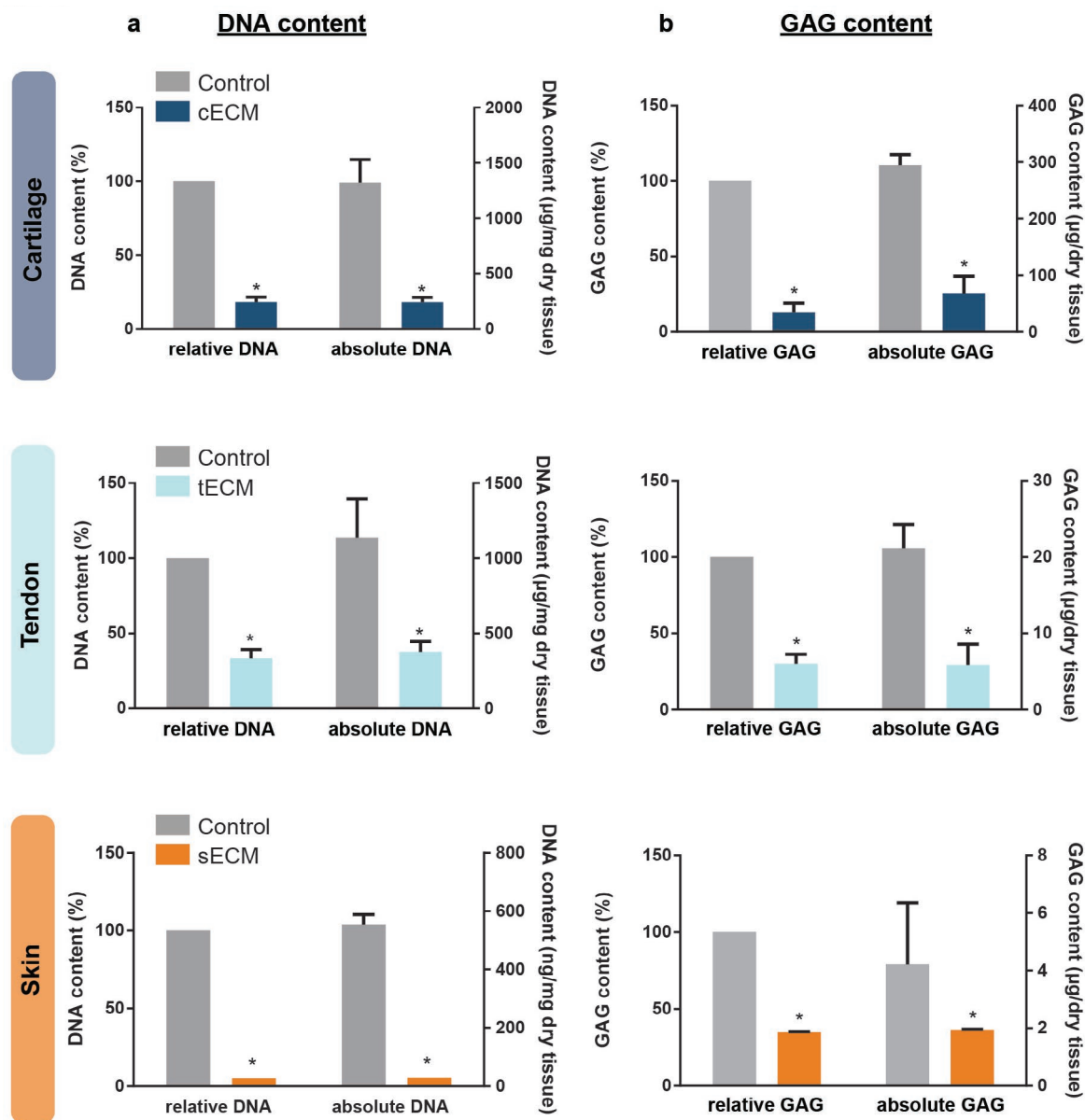


Fig. 4. DNA and GAG content before (control) and after treatment (decellularised). (a) Relative (normalised) and absolute DNA content; (b) relative (normalised) and absolute GAG content. * $p < 0.05$.

bovine chondrocytes was limited to the surface of all decellularised tissues types (Fig. 7, middle). Furthermore, chondrocytes remained viable after 1 week, as seen by a constant fluorescent signal in the PrestoBlue™ assay (Fig. 7, bottom).

Discussion

The working hypothesis of the present study was that scCO₂ might be optimised to decellularise dense tissues in combination with a CO₂-philic detergent. To verify this hypothesis, experiments with scCO₂ on articular cartilage, tendons and skin were performed.

Decellularisation with scCO₂ and a CO₂-philic detergent only, could not achieve a complete decellularisation of cartilage and skin. Thus, additional steps were introduced. For cartilage, an extensive pre-treatment involving freeze-thaw,

osmotic shock and enzymatic digestion was needed to achieve effective decellularisation. For skin, the pre-treatment consisted of removing the epidermis prior to decellularisation.

The described method substantially reduced the cellular material in all dense tissue types tested (Fig. 2a-c). From a visual inspection, there were virtually no cell nuclei in the H&E staining as compared to the native tissue, which was confirmed by the significantly reduced DNA content (* $p < 0.05$) (Fig. 4a). There were only trace amounts of broken cell nuclei visible in the DAPI staining.

For cartilage, a DNA reduction from 1321 ± 210 ng to 241 ± 45 ng dsDNA/mg dry tissue (reduced by 82 ± 3 %) was achieved (Fig. 4a), compared to the 47.6 ng dsDNA/mg dry tissue (reduced by 94 %) achieved by Bautista *et al.* (2016). In tendons, the DNA content was reduced from 1135 ± 262 ng to 378 ± 68 ng dsDNA/mg dry tissue (reduced by 67 ± 6 %) (Fig. 4a)

as compared to the ~ 100 ng/mg dry tissue (reduced by 90 %) achieved by Xu *et al.* (2017). For skin, a reduction from 554 ± 34 ng to 29 ± 0.05 ng dsDNA/mg dry tissue (reduced by 95 ± 0.004 %) was observed (Fig. 4a), compared to 40 ng dsDNA/mg dry tissue obtained by Zhang *et al.* (2016). It should be noted that the DNA content in the native tissues was higher per mg dry tissue than in the cited studies. This could be due to batch-to-batch variation and differences in the DNA extraction method.

Comparing the absolute DNA content achieved with the technique here described to the threshold defined by Crapo and *et al.* (2011), only skin was below the limit of 50 ng dsDNA/mg dry tissue, whereas cartilage and tendons contained substantially more DNA. GAG content was significantly reduced ($p < 0.05$) in cartilage, in tendons and in skin (Fig. 4b).

This was consistent with previous studies reporting a GAG reduction by 71.0 ± 6.10 % in cartilage (Bautista *et al.*, 2016) and 67 % in tendons (Youngstrom *et al.*, 2013) using a SDS-based decellularisation protocol. For skin, 1.56 ± 0.42 $\mu\text{g}/\text{mg}$ GAG/dry weight are retained in the decellularised dermis according to Zhang *et al.* (2016), being less than what was retained using the here presented protocol. However, Zhang *et al.* (2016) do not perform any comparison with the native tissue.

It should be noted that decellularisation does not always remove a significant amount of GAGs. For instance, decellularisation of rat hearts with SDS in pulsatile flow retains most of the GAGs in the ECM (Park *et al.*, 2018). Likewise, optimisation of the decellularisation protocol can significantly enhance the remaining GAG content in a decellularised

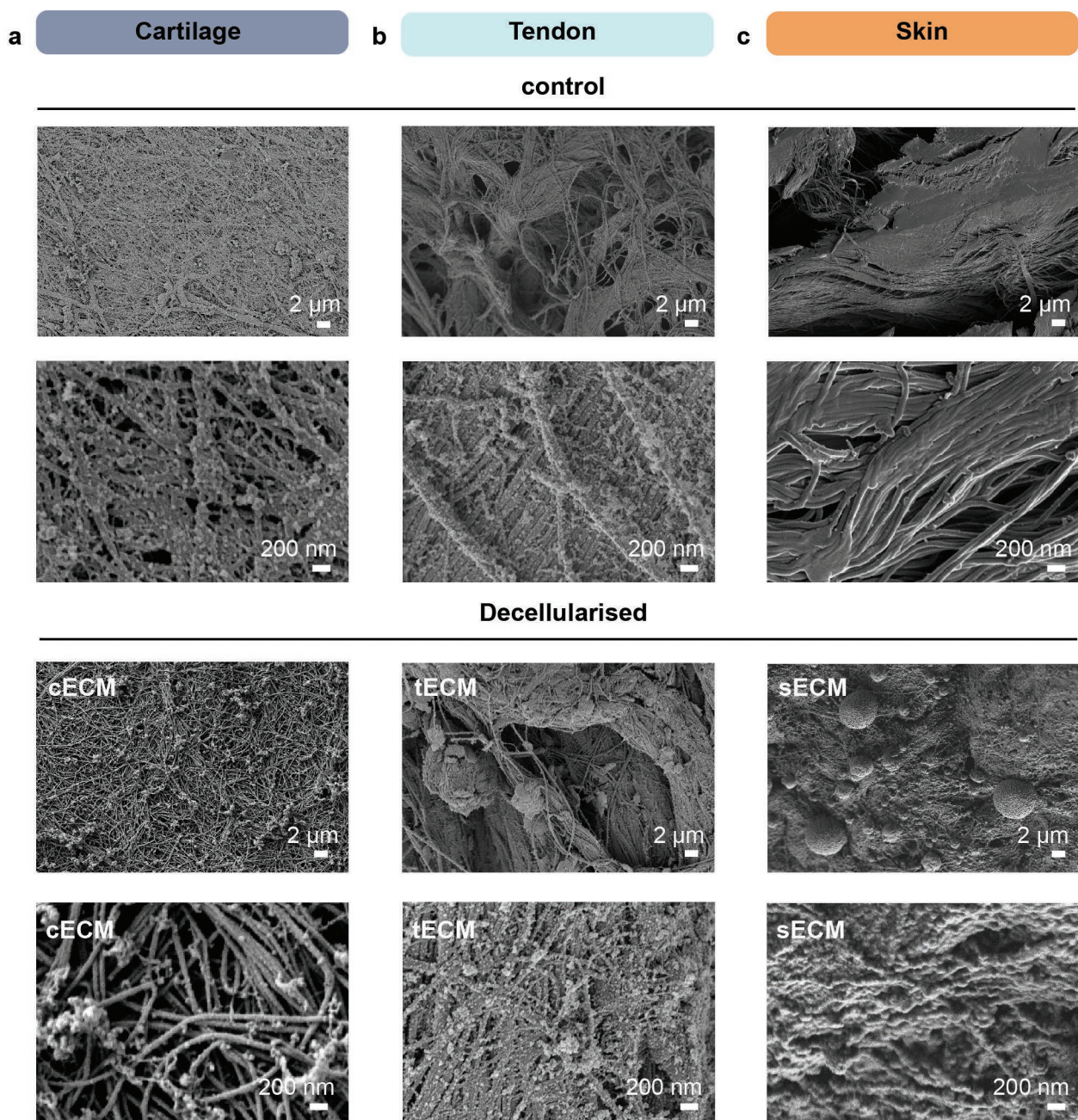


Fig. 5. Ultrastructure of cartilage, tendon and skin. (a) Bovine cartilage (top view-superficial layer), (b) horse tendon (top view), (c) human skin (cross-section); scale bar: 2 μm and 200 nm, respectively.

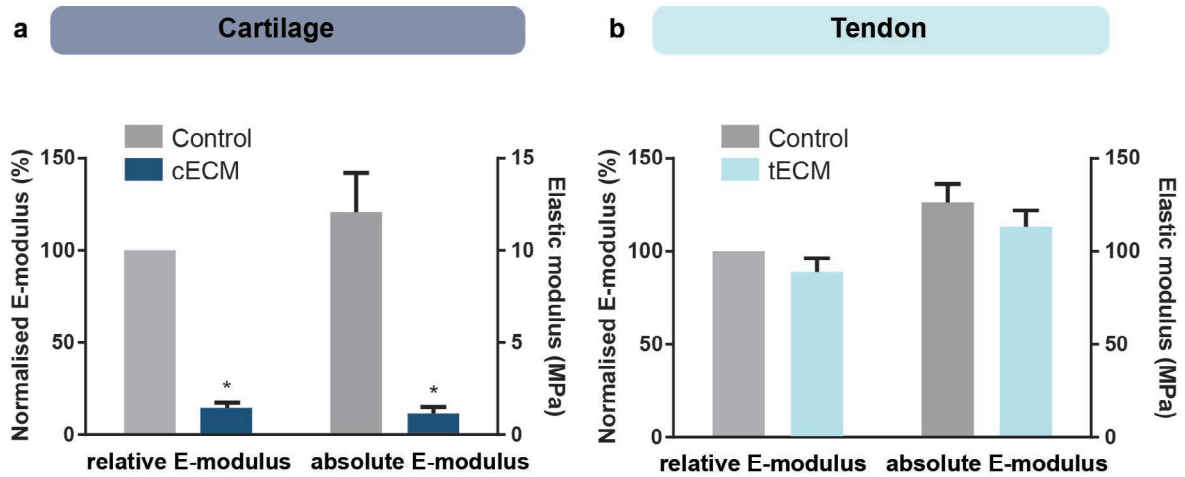


Fig. 6. Elastic modulus of cartilage and tendon after the decellularisation treatment. (a) Compression test of bovine cartilage at 200 $\mu\text{m/s}$ loading rate (elastic modulus normalised to the native tissue in percentage and absolute values in MPa), $n = 4$ samples per condition; (b) tension test of horse tendon at 0.1 mm/s (elastic modulus normalised to the native tissue in percentage and absolute values in MPa), $n = 4$ samples per condition, $*p < 0.0001$.

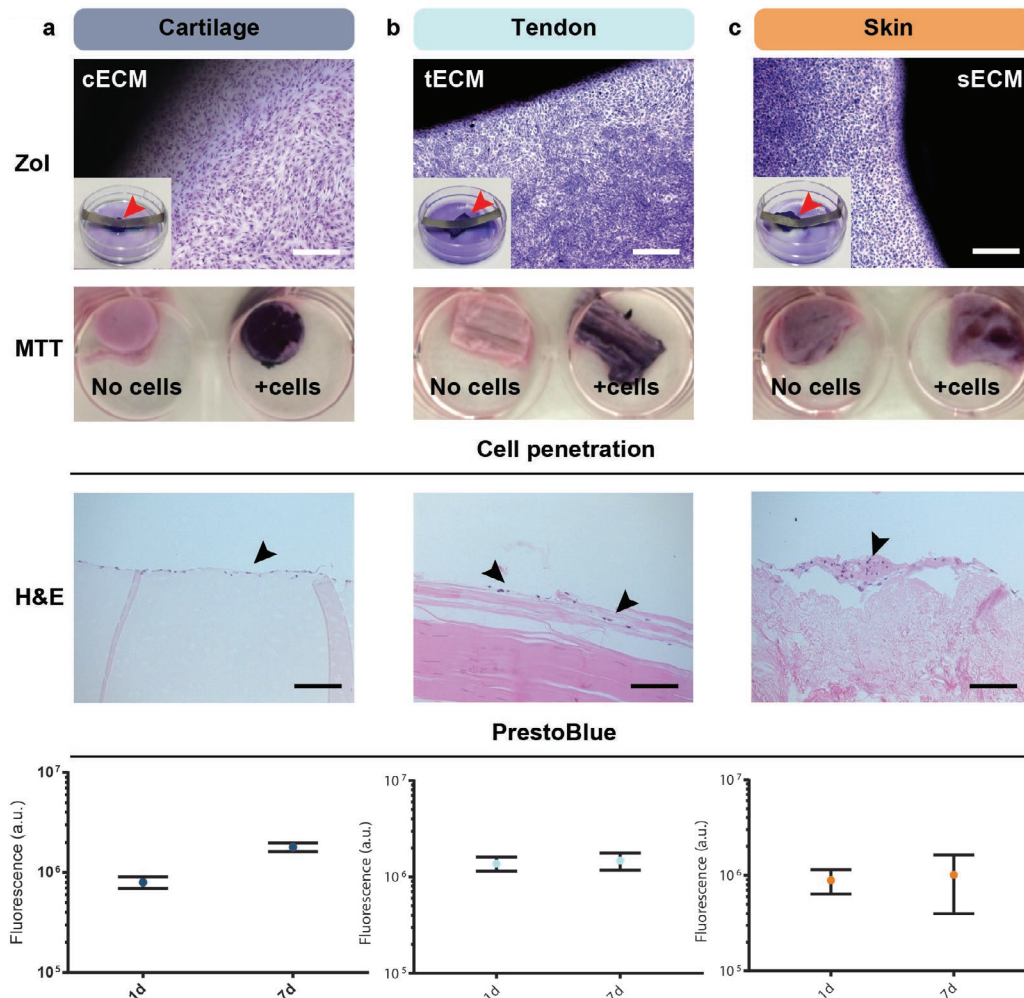


Fig. 7. Biocompatibility of decellularised tissues. (Top) ZoL of (a) bovine cartilage, (b) horse tendon and (c) human skin after 1 d; red arrows indicate location of decellularised tissue; scale bar: 400 μm . (Middle) MTT assay after 7 d of cell culture (control without seeded cells); H&E staining showing cell penetration of bovine chondrocytes after 7 d of culture on c-, t- and sECM, scale bar: 200 μm . (Bottom) PrestoBlue™ assay showed constant fluorescent signal (in arbitrary units: a.u.) after 7 d of cell culture (in each test $n = 3$ samples per condition).

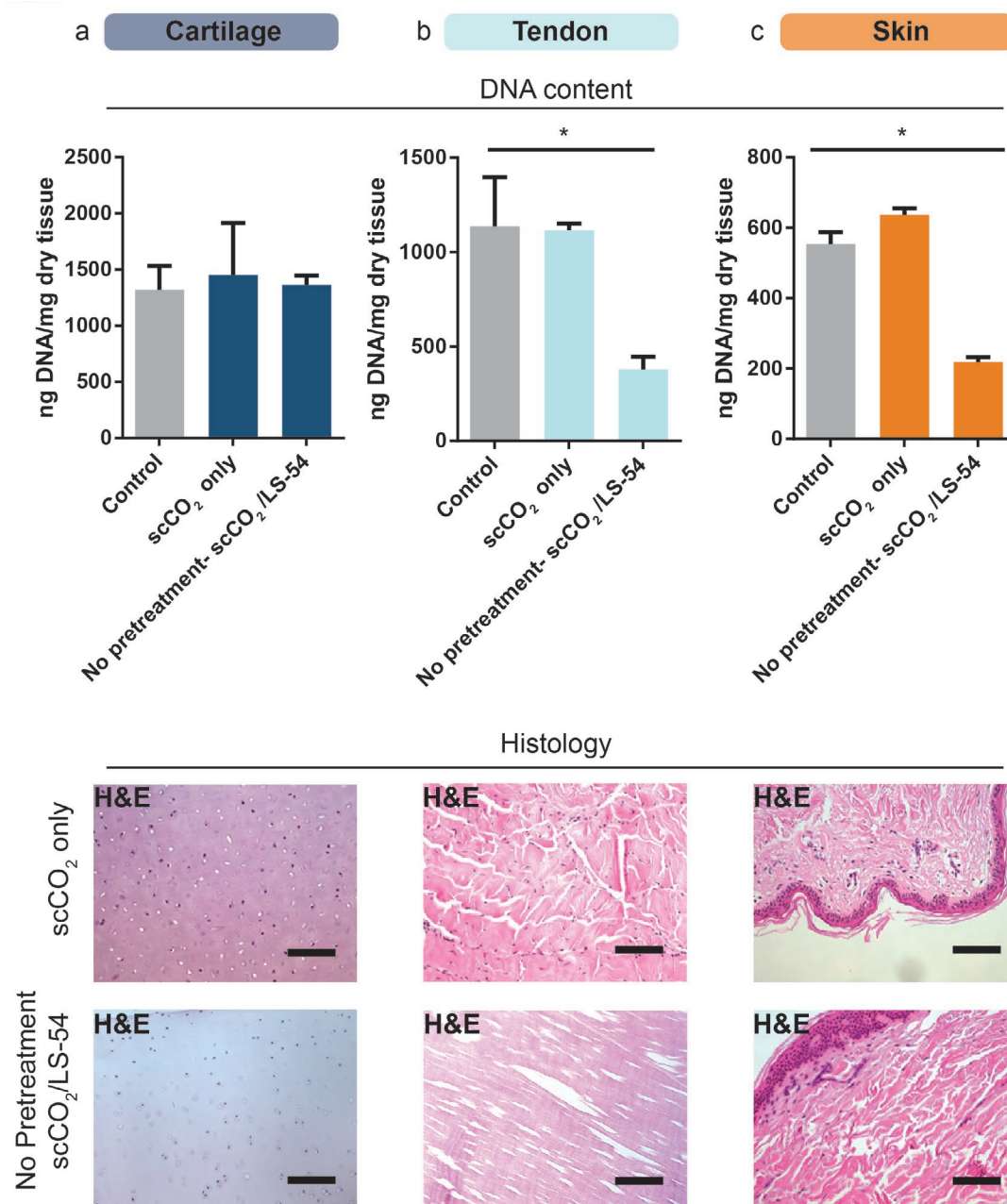


Fig. 8. Effect of scCO₂ and pre-treatment. Upper part indicates DNA content in ng/mg dry tissue whereas lower part illustrates visual cell nuclei by H&E staining; (a) cartilage; (b) tendon; (c) skin; * $p < 0.05$; scale bar: 200 μm.

nucleus pulposus (Illien-Jünger *et al.*, 2016). GAGs are important for the visco-elastic properties of tissues (Lovekamp *et al.*, 2006). The GAG reduction was a possible explanation for the looser arrangement of collagen fibres in the ultrastructure of articular cartilage after decellularisation (Fig. 5a). Therefore, the present study supported the results of Schneider *et al.* (2016), who show a looser collagen fibre arrangement in articular cartilage after decellularisation. Moreover, the less dense fibre arrangement results in a higher porosity, which is a potential advantage for the recellularisation of decellularised tissues (Nasrollahzadeh *et al.*, 2017).

The cell adhesion molecules, fibronectin and laminin, were still present in the tissues after the

decellularisation procedure (Fig. 3). Although, it should be noted that laminin was mostly present in close vicinity to blood vessels and in the pericellular space. A comparison of the results of this study with the previously cited decellularisation studies of articular cartilage (Bautista *et al.*, 2016; Schneider *et al.*, 2016) and tendons (Xu *et al.*, 2017; Youngstrom *et al.*, 2013) was not possible, since no immunohistochemistry was performed in these studies. Only in case of the Zhang *et al.* (2016) study, immunohistochemistry was performed and, similar to the observations of the present study, laminin was detected around the blood vessels. The conservation of cell adhesion molecules after the decellularisation process was a positive result, since cell adhesion molecules are crucial for

the bioactivity of the decellularised tissue. For this reason, cell adhesion molecules (fibronectin, laminin, arginyglycylaspartic-acid-containing molecules and others) are often added to synthetic materials to enhance their bioactivity (Lutolf and Hubbell, 2005; Shin *et al.*, 2003).

Mechanical tests showed that the stiffness of the decellularised tissues was not affected by the treatment in case of tendons but dropped significantly ($*p < 0.0001$) in articular cartilage (Fig. 6). These results compared well with other studies in which equine tendons and porcine articular cartilage are decellularised by SDS. For equine tendons, the elastic modulus decreases from 76.13 ± 4.12 MPa to 70.31 ± 5.91 MPa [92.35 ± 8.41 % of the native tendons elastic modulus is maintained (Youngstrom *et al.*, 2013)]; for porcine articular cartilage, the equilibrium modulus is reduced from 0.145 MPa to 0.035 MPa [maintaining 24.8 ± 2.2 % of the native cartilage properties (Bautista *et al.*, 2016)]. In the described protocol, the reduction in elastic modulus of the articular cartilage could be caused by the extensive pre-treatment, which removed most GAG molecules from the ECM. A loss of GAGs, which attracts water into the ECM, affects the mechanical properties of tissues through a loss of hydrostatic pressure (Bautista *et al.*, 2016; Maroudas *et al.*, 1969; Maroudas, 1976). For tendons, the effect of a lower GAG content is less pronounced since tendons only contain between 0.2 % and 5 % GAGs in the tensional zone and in the dry mass at the bone insertion area, respectively (Merrilees and Flint, 1980). Since tendons mostly work in tension and not in compression, GAG content is less important than in articular cartilage, where 11 % of GAGs in dry mass can be detected (Yu *et al.*, 1997).

The decellularised tissues were non-cytotoxic to bovine chondrocytes (Fig. 7) and human tenocytes and fibroblasts (data not shown). The biocompatibility was further evidenced by ZoI, MTT and PrestoBlue™ assays after 1 week of culture. The cell penetration of bovine chondrocytes into the decellularised tissues was mostly limited to the surface of the tissue (Fig. 7, middle) after 1 week of cell culture. However, these tests are only a first indicator for a favourable biocompatibility. More extensive studies attempting to recellularise the obtained decellularised tissues should also be performed for a final confirmation of biocompatibility.

The effect of scCO₂ only and of pre-treatment on the DNA content of cartilage, tendons and skin are displayed in Fig. 8. scCO₂ only did not reduce the DNA content in any of the three tissues. This was expected since scCO₂ itself is apolar and needs a co-solvent such as ethanol or a CO₂-philic detergent to remove polar molecules such as phospholipids (cell membrane) or DNA (Dunford and Temelli, 1995; Montanari *et al.*, 1999; Tanaka *et al.*, 2004). Without pre-treatment, scCO₂/LS-54 could significantly reduce the DNA content of tendons ($p < 0.05$). However, to effectively remove DNA content and visual cell

nuclei, cartilage and skin required a pre-treatment prior to treatment with scCO₂/LS-54. It is possible that a pre-treatment of articular cartilage was necessary due to the high density of its ECM with an average pore size of only 6 nm (Maroudas, 1973). Hence, to effectively remove phospholipids and DNA, a pre-treatment to loosen the ECM structure was required for cartilage. Without a pre-treatment, the DNA content of skin was significantly reduced ($p < 0.05$), but visual cell nuclei remained as displayed in Fig. 8c. Thus, the epidermis was removed prior to treatment with scCO₂/LS-54.

The present study had also several inherent limitations. Decellularisation of cartilage and skin required a pre-treatment since scCO₂ and CO₂-philic detergent could not completely decellularise these tissues. The pre-treatment significantly reduced the mechanical properties of articular cartilage. One possible solution to enhance the efficiency of the scCO₂ and CO₂-philic detergent decellularisation and to avoid these aggressive pre-treatment steps is a modification of the process parameters such as pressure, treatment time, temperature and concentration of detergent. A higher process pressure (not possible with the autoclave used) could help to entirely remove the CO₂-philic detergent LS-54 by simple rinsing with scCO₂. With the current protocol, decellularised tissues still contained residual detergent and required an additional washing step in PBS to obtain a high biocompatibility. The detergent Dehypon® LS-54 is a common household and industrial surfactant, which has a high toxicity for aquatic organisms according to its safety data sheet. Hence, when used for decellularisation, LS-54 should be completely removed to avoid cytotoxicity. In preliminary tests of different doses of LS-54 in DMEM, a concentration as low as 0.01 % demonstrated toxicity on bovine chondrocytes. Living chondrocytes were observed at a concentration of 0.002 % (data not shown). Thus, a complete removal of LS-54 is paramount. Trace amounts of this detergent can be detected by analytical methods such as nuclear magnetic resonance (NMR) (Juansilfero *et al.*, 2011). Thus, it would be possible to use NMR to evaluate the successful removal of the detergent LS-54 from the decellularised tissues.

The size of the diverse decellularised tissues was different. This was due to the distinct processing steps of each tissue and different available tissue sources. However, the use of a supercritical fluid should also enable the use of bigger samples since diffusion is largely enhanced.

One aspect that was not verified completely during this study was the sterility of the decellularised tissues after scCO₂ treatment. scCO₂ can be used as a gentle sterilisation technique for tissues (Bernhardt *et al.*, 2015). For instance, scCO₂ is used to sterilise tendons whereby mechanical properties are maintained (Nichols *et al.*, 2009). However, if sterility was also achievable with the used protocol was not tested. This should ideally be done after a further

optimisation of the protocol. However, the fact that cells were cultured with the treated matrix for the biocompatibility assay and no contamination was observed would indicate that the matrix was sterile. Despite these limitations, the scCO₂ and CO₂-philic detergent decellularisation protocol worked well for tendons that were decellularised without any pre-treatment, while maintaining most of their mechanical properties. The protocols for skin and cartilage were not perfected yet as additional treatment steps were still necessary for decellularisation; however, there is still room for improvement by using a more powerful autoclave. Also, important cell adhesion molecules such as fibronectin and laminin were preserved in the ECM of all tested tissues after the procedure, an important aspect that was widely neglected in earlier publications. The focus of future experiments should be a further optimisation of the process parameters for all tissues, a substantial reduction of pre- and post-treatment steps for skin and cartilage and complete sterility testing. Taken together, the use of scCO₂ and CO₂-philic detergent had advantages when compared to established methods for the decellularisation of tendons. With further optimisation of the process parameters, it could also become a true alternative for other dense tissues, including skin and cartilage.

Acknowledgements

We would like to thank the Swiss National Science Foundation (#200021_150190 and #IZLCZ3_156126) and the Lausanne Orthopaedic Research Foundation (LORF) for their financial support. P.A. was supported by a MD-PhD Leenaards grant. Additionally, we thank Sandra Jaccoud and Dr Virginie Philippe for assistance with the DAL Biobank and Maxence Volz and Cédric Peneverye for their work on the skin decellularisation. Furthermore, we would like to thank Valérie Malfroy Camine for her precious help with the data visualisation.

No competing financial interests exist.

References

Aubin H, Kranz A, Hülsmann J, Lichtenberg A, Akhyari P (2013) Decellularized whole heart for bioartificial heart. *Methods Mol Biol* **1036**: 163-178.

Badylak SF, Hoppo T, Nieponice A, Gilbert TW, Davison JM, Jobe BA (2011) Esophageal preservation in five male patients after endoscopic inner-layer circumferential resection in the setting of superficial cancer: a regenerative medicine approach with a biologic scaffold. *Tissue Eng Part A* **17**: 1643-1650.

Bautista CA, Park HJ, Mazur CM, Aaron RK, Bilgen B (2016) Effects of chondroitinase ABC-mediated proteoglycan digestion on decellularization and recellularization of articular cartilage. *PLoS One* **11**: 1-15.

Bernhardt A, Wehrl M, Paul B, Hochmuth T, Schumacher M, Schütz K, Gelinsky M (2015) Improved sterilization of sensitive biomaterials with supercritical carbon dioxide at low temperature. *PLoS One* **10**: e0129205. DOI: 10.1371/journal.pone.0129205.

Caione P, Boldrinic R, Salerno A, Nappo SG (2012) Bladder augmentation using acellular collagen biomatrix: a pilot experience in exstrophic patients. *Pediatr Surg Int* **28**: 421-428.

Casali DM, Handleton RM, Shazly T, Matthews MA (2018) A novel supercritical CO₂-based decellularization method for maintaining scaffold hydration and mechanical properties. *J Supercrit Fluids* **131**: 72-81.

Crapo PM, Gilbert TW, Badylak SF (2011) An overview of tissue and whole organ decellularization processes. *Biomaterials* **32**: 3233-3243.

Dunford NT, Temelli F (1995) Extraction of phospholipids from canola with supercritical carbon dioxide and ethanol. *J Am Oil Chem Soc* **72**: 1009-1015.

Freytes DO, Stoner RM, Badylak SF (2008) Uniaxial and biaxial properties of terminally sterilized porcine urinary bladder matrix scaffolds. *J Biomed Mater Res B Appl Biomater* **84**: 408-414.

Guler S, Aslan B, Hosseinian P, Aydin HM (2017) Supercritical carbon dioxide-assisted decellularization of aorta and cornea. *Tissue Eng Part C Methods* **23**: 540-547.

Halfwerk FR, Rouwkema J, Gossen JA, Grandjean JG (2018) Supercritical carbon dioxide decellularised pericardium: mechanical and structural characterisation for applications in cardio-thoracic surgery. *J Mech Behav Biomed Mater* **77**: 400-407.

Hodde J, Hiles M (2002) Virus safety of a porcine-derived medical device: evaluation of a viral inactivation method. *Biotechnol Bioeng* **79**: 211-216.

Huang Y, Tseng F, Chang W, Peng I, Hsieh D, Wu S (2017) Preparation of acellular scaffold for corneal tissue engineering by supercritical carbon dioxide extraction technology. *Acta Biomater* **58**: 238-243.

Illien-Jünger S, Sedaghatpour DD, Laudier DM, Hecht AC, Qureshi SA, Iatridis JC (2016) Development of a bovine decellularized extracellular matrix-biomaterial for nucleus pulposus regeneration. *J Orthop Res* **34**: 876-888.

Juanssilfero AB, Akmal F, Mutalib A, Zulaikha W, Zulkifli W, Jahim J (2011) Characterization of copolymer Dehypon® LS 54 and its application for aqueous two-phase systems paired with the waxy maize starch for protein extraction. *IJASEIT*: DOI: 10.18517/ijaseit.1.1.16.

Liu J, Han B, Zhang J, Li G, Zhang X, Wang J, Dong B (2002) Formation of water-in-CO₂ microemulsions with non-fluorous surfactant Ls-54 and solubilization of biomacromolecules. *Chemistry* **8**: 1356-1360.

Lovekamp JJ, Simionescu DT, Mercuri JJ, Zubieta B, Sacks MS, Vyavahare NR (2006) Stability and function of glycosaminoglycans in porcine bioprosthesis heart valves. *Biomaterials* **27**: 1507-1518.

- Lutolf MP, Hubbell JA (2005) Synthetic biomaterials as instructive extracellular microenvironments for morphogenesis in tissue engineering. *Nat Biotechnol* **23**: 47-55.
- Macchiarini P, Jungebluth P, Go T, Asnaghi MA, Rees LE, Cogan TA, Dodson A, Martorell J, Bellini S, Parnigotto PP, Dickinson SC, Hollander AP, Mantero S, Conconi MT, Birchall MA (2008) Clinical transplantation of a tissue-engineered airway. *Lancet* **372**: 2023-2030.
- Maroudas AI (1976) Balance between swelling pressure and collagen tension in normal and degenerate cartilage. *Nature* **260**: 808-809.
- Maroudas A (1973) Physico-chemical properties of articular cartilage. In: *Adult Articular Cartilage* Ed: MAR Freeman, London Pitman Medical, pp: 131-170.
- Maroudas A, Muir H, Wingham J (1969) The correlation of fixed negative charge with glycosaminoglycan content of human articular cartilage. *Biochim Biophys Acta* **177**: 492-500.
- Merrilees MJ, Flint MH (1980) Ultrastructural study of tension and pressure zones in a rabbit flexor tendon. *Am J Anat* **157**: 87-106.
- Montanari L, Fantozzi P, Snyder JM, King JW (1999) Selective extraction of phospholipids from soybeans with supercritical carbon dioxide and ethanol. *J Supercrit Fluids* **14**: 87-93.
- Nasrollahzadeh N, Applegate LA, Pioletti DP (2017) Development of an effective cell seeding technique: simulation, implementation, and analysis of contributing factors. *Tissue Eng Part C Methods* **23**: 485-496.
- Nichols A, Burns DC, Christopher R (2009) Studies on the sterilization of human bone and tendon musculoskeletal allograft tissue using supercritical carbon dioxide. *J Orthop* **6**: e9.
- Nourissat G, Berenbaum F, Duprez D (2015) Tendon injury: from biology to tendon repair. *Nat Rev Rheumatol* **11**: 223-233.
- Ott HC, Clippinger B, Conrad C, Schuetz C, Pomerantseva I, Ikononou L, Kotton D, Vacanti JP (2010) Regeneration and orthotopic transplantation of a bioartificial lung. *Nat Med* **16**: 927-933.
- Ott HC, Matthiesen TS, Goh S-K, Black LD, Kren SM, Netoff TI, Taylor D a (2008) Perfusion-decellularized matrix: using nature's platform to engineer a bioartificial heart. *Nat Med* **14**: 213-221.
- Park SM, Yang S, Rye SM, Choi SW (2018) Effect of pulsatile flow perfusion on decellularization. *Biomed Eng Online* **17**: 15. DOI: 10.1186/s12938-018-0445-0.
- Patton JH, Berry S, Kralovich KA (2007) Use of human acellular dermal matrix in complex and contaminated abdominal wall reconstructions. *Am J Surg* **193**: 360-363.
- Petersen THT, Calle EAE, Zhao L, Lee EJ, Gui L, Raredon MB, Gavrilov K, Yi T, Zhuang ZW, Breuer C, Herzog E, Niklason LE (2010) Tissue-engineered lungs for *in vivo* implantation. *Science* **329**: 538-541.
- Raghavan SS, Woon CYL, Kraus A, Megerle K, Choi MSS, Pridgen BC, Pham H, Chang J (2012) Human flexor tendon tissue engineering: decellularization of human flexor tendons reduces immunogenicity *in vivo*. *Tissue Eng Part A* **18**: 796-805.
- Rosario DJ, Reilly GC, Ali Salah E, Glover M, Bullock AJ, Macneil S (2008) Decellularization and sterilization of porcine urinary bladder matrix for tissue engineering in the lower urinary tract. *Regen Med* **3**: 145-156.
- Sawada K, Terada D, Yamaoka T, Kitamura S, Fujisato T (2008) Cell removal with supercritical carbon dioxide for acellular artificial tissue. *J Chem Technol Biotechnol* **83**: 943-949
- Schneider C, Lehmann J, van Osch GJVM, Hildner F, Teuschl A, Monforte X, Miosga D, Heimel P, Priglinger E, Redl H, Wolbank S, Nürnberger S (2016) Systematic comparison of protocols for the preparation of human articular cartilage for use as scaffold material in cartilage tissue engineering. *Tissue Eng Part C Methods* **22**: 1095-1107.
- Shin H, Jo S, Mikos AG (2003) Biomimetic materials for tissue engineering. *Biomaterials* **24**: 4353-4364.
- Song JJ, Guyette JP, Gilpin SE, Gonzalez G, Vacanti JP, Ott HC (2013) Regeneration and experimental orthotopic transplantation of a bioengineered kidney. *Nat Med* **19**: 646-651.
- Sun WQ, Leung P (2008) Calorimetric study of extracellular tissue matrix degradation and instability after gamma irradiation. *Acta Biomater* **4**: 817-826.
- Sutherland AJ, Converse GL, Hopkins RA, Detamore MS (2014) The bioactivity of cartilage extracellular matrix in articular cartilage regeneration. *Adv Healthc Mater* **4**: 29-39.
- Tanaka Y, Sakaki I, Ohkubo T (2004) Extraction of phospholipids from salmon roe with supercritical carbon dioxide and an entrainer. *J Oleo Sci* **53**: 417-424.
- Uygun BE, Soto-Gutierrez A, Yagi H, Izamis M-L, Guzzardi MA, Shulman C, Milwid J, Kobayashi N, Tilles A, Berthiaume F, Hertl M, Nahmias Y, Yarmush ML, Uygun K (2010) Organ reengineering through development of a transplantable recellularized liver graft using decellularized liver matrix. *Nat Med* **16**: 814-820.
- Wainwright JM, Czajka CA, Patel UB, Freytes DO, Tobita K, Gilbert TW, Badylak SF (2010) Preparation of cardiac extracellular matrix from an intact porcine heart. *Tissue Eng Part C Methods* **16**: 525-532.
- Wang JK, Luo B, Guneta V, Li L, Foo SEM, Dai Y, Tan TTY, Tan NS, Choong C, Wong MTC (2017) Supercritical carbon dioxide extracted extracellular matrix material from adipose tissue. *Mater Sci Eng C* **75**: 349-358.
- Xu K, Kuntz LA, Foehr P, Kuempel K, Wagner A, Tuebel J, Deimling C V., Burgkart RH (2017) Efficient decellularization for tissue engineering of the tendon-bone interface with preservation of biomechanics. *PLoS One* **12**: e0171577. DOI: 10.1371/journal.pone.0171577.
- Yang Z, Shi Y, Wei X, He J, Yang S, Dickson G, Tang J, Xiang J, Song C, Li G (2010) Fabrication and repair

of cartilage defects with a novel acellular cartilage matrix scaffold. *Tissue Eng Part C Methods* **16**: 865-876.

Youngstrom DW, Barrett JG, Jose RR, Kaplan DL (2013) Functional characterization of detergent-decellularized equine tendon extracellular matrix for tissue engineering applications. *PLoS One* **8**: e64151. DOI: 10.1371/journal.pone.0064151.

Yu H, Grynepas M, Kandel RA (1997) Composition of cartilagenous tissue with mineralized and non-mineralized zones formed *in vitro*. *Biomaterials* **18**: 1425-1431.

Zambon A, Vetralla M, Urbani L, Pantano MF, Ferrentino G, Pozzobon M, Pugno NM, Coppi P De, Elvassore N, Spilimbergo S (2016) Dry acellular oesophageal matrix prepared by supercritical carbon dioxide. *J Supercrit Fluids* **115**: 33-41.

Zhang Q, Johnson JA, Dunne LW, Chen Y, Iyyanki T, Wu Y, Chang EI, Branch-Brooks CD, Robb GL, Butler CE (2016) Decellularized skin/adipose tissue flap matrix for engineering vascularized composite soft tissue flaps. *Acta Biomater* **35**: 166-184.

Discussion with Reviewers

Baldini Nicola: Two arguable flaws of the publication were: 1) content of DNA was still higher than other methods; 2) pre-treatment of cartilage was a bit rough and required many steps. Can the authors comment on these?

Authors: 1) The DNA content could be further reduced by several means. First, the pressure in the autoclave could be increased to enhance the decellularisation (a different autoclave would be required). Secondly, other substances could be added in the autoclave, such as peracetic acid or hydrogen peroxide, which are used as additive to scCO₂ for sterilising tendon and bone (Nichols *et al.*, 2009). Finally, nucleases are used to digest the DNA, demonstrating a reduction below 50 ng dsDNA/mg dry tissue (Bautista *et al.*, 2016; Xu *et al.*, 2017). Incorporating the aforementioned suggestions within the described model could reduce the DNA content below 50 ng dsDNA/mg dry tissue.

2) Cartilage decellularisation is particularly difficult due to the high density of its ECM, with only 6 nm-diameter average pore size (Maroudas, 1973). Hence, for efficient decellularisation, the ECM needs to be loosened to access the cellular material and DNA. In the presented protocol, the described additional steps were necessary for decellularisation of the dense articular cartilage ECM.

Bahar Bilgen: One of the major challenges in tissue decellularisation is the ability to recellularise the tissues. Had the cells infiltrated the decellularised matrix after 7 d of culture on the decellularised ECM?
Authors: Yes, the cells could infiltrate the tissues

after 7 d, however, the infiltration depth was mostly limited to the surface (Fig. 7). To enhance the depth of cell penetration, the cell culture time should be prolonged.

Bahar Bilgen: How do you explain that using scCO₂ seemed to remove more GAGs and less DNA as compared to other studies on similar tissues?

Authors: Using other decellularisation techniques, a high GAG content can be maintained, while DNA is effectively removed (Park *et al.*, 2018). However, in the present case, the GAG content was diminished, while DNA content remained on a comparatively high level. It is possible that the lower GAG content as compared to the DNA content was due to higher solvability of GAGs in scCO₂/LS-54 than phospholipids and DNA.

Anne Bernhardt: Do you think there are alternatives to the CO₂-philic reagent LS-54, which are easier to remove from the samples after decellularisation?

Authors: Yes, there are multiple detergents that are solvable in scCO₂, including expensive fluorinated detergents, sugar acetate and CO₂-philic hydrocarbons (Fink *et al.*, 1999; Raveendran and Wallen, 2002; Sarbu *et al.*, 2000, additional references). However, the LS-54 was used because it is an easily accessible commercial product and, thus, economically affordable. Moreover, the effect of the aforementioned LS-54 alternatives on important experimental outcomes, such as biocompatibility, would have to be studied. Finally, a more ideal case would be the use of ethanol as co-solvent since ethanol can be more easily removed from the tissue. However, using ethanol as co-solvent in the setup used did not decellularise the tested tissues. Hence, a new strategy involving a CO₂-philic detergent such as LS-54 was developed. Using ethanol as co-solvent might still be a viable option, but this would have to be tested in a setup that can attain higher pressures.

Additional References

Fink R, Hancu D, Valentine R, Beckman EJ (1999) Toward the development of "CO₂-philic" hydrocarbons. 1. Use of side-chain functionalization to lower the miscibility pressure of polydimethylsiloxanes in CO₂. *J Phys Chem B* **103**: 6441-6444.

Raveendran P, Wallen SL (2002) Sugar acetates as novel, renewable CO₂-philes. *J Am Chem Soc* **124**: 7274-7275.

Sarbu T, Styranc T, Beckman EJ (2000) Design and synthesis of low cost, sustainable CO₂-philes. *Ind Eng Chem Res* **39**: 4678-4683.

Editor's note: The Scientific Editor responsible for this paper was Juerg Gasser.